Synthetic and Systems Biotechnology 7 (2022) 887–899

Contents lists available at ScienceDirect

Synthetic and Systems Biotechnology

journal homepage: www.keaipublishing.com/en/journals/synthetic-and-systems-biotechnology

Current state and future perspectives of cytochrome P450 enzymes for C–H and C=C oxygenation

Yu Yan [a,b], Jing Wu [b], Guipeng Hu [b], Cong Gao [a], Liang Guo [a], Xiulai Chen [a], Liming Liu [a], Wei Song [b,*]

[a] State Key Laboratory of Food Science and Technology, Jiangnan University, Wuxi, 214122, China
[b] School of Life Sciences and Health Engineering, Jiangnan University, Wuxi, 214122, China

ARTICLE INFO

Keywords:
Biocatalysis
P450 enzymes
C–H and C=C oxygenation

ABSTRACT

Cytochrome P450 enzymes (CYPs) catalyze a series of C–H and C=C oxygenation reactions, including hydroxylation, epoxidation, and ketonization. They are attractive biocatalysts because of their ability to selectively introduce oxygen into inert molecules under mild conditions. This review provides a comprehensive overview of the C–H and C=C oxygenation reactions catalyzed by CYPs and the various strategies for achieving higher selectivity and enzymatic activity. Furthermore, we discuss the application of C–H and C=C oxygenation catalyzed by CYPs to obtain the desired chemicals or pharmaceutical intermediates in practical production. The rapid development of protein engineering for CYPs provides excellent biocatalysts for selective C–H and C=C oxygenation reactions, thereby promoting the development of environmentally friendly and sustainable production processes.

1. Background

Direct C–H and C=C oxygenation reactions that avoid the prefunctionalization step lead to the formation of carbon-oxygen bonds and are indispensable in synthesizing pharmaceutical intermediates and chemicals [1,2]. As carbon is more stable and common in complex compounds, its oxygenation reactions have become a research hotspot. Industrial-scale C–H and C=C oxygenation is achieved through the Hock process [3], Dakin oxidation [4] cooperated with Vilsmeier–Haack formylation [5], and various transition metal-catalyzed reactions [6], including C–O bond formation promoted by palladium [7], Sandmeyer hydroxylation [8], and Chan–Lam couplings [9]. Most C–H and C=C oxygenation reactions are performed on molecules with specific functional groups that can be transformed into -oxy substituents, such as aryl halides [10] and aryl thianthrenium salts [3]. However, how substrate molecules without special functional groups efficiently achieve selective C–H and C=C oxygenation reactions is a crucial problem in producing high value-added chemicals.

As a class of multifunctional metalloenzymes, cytochrome P450 enzymes (CYPs) have attracted recent attention. They have been extensively studied owing to their excellent catalytic capacity, various reaction types, and broad substrate range. CYPs catalyze a wide range of reactions, such as N/S-oxidation, N/O/S-dealkylation, C–C bond cleavage, epoxidation of C=C bonds, hydroxylation, and ketonization of C–H bonds, thereby having excellent application potential for medicine, food processing, chemistry, and other fields [11,12]. Unlike most oxidases, CYPs can catalyze the hydroxylation of saturated alkanes without requiring any special groups and active elements and quickly activate inert molecules by using O_2 or H_2O_2, which has high economic significance for chemical production based on simple raw materials [13,14]. Furthermore, the epoxidation of carbon-carbon unsaturated bonds is a typical C=C oxygenation reaction catalyzed by CYPs, which not only accomplishes the insertion of oxygen atoms but also achieves ring formation by overcoming tension and other factors [15,16]. Surprisingly, a few CYPs can further catalyze the ketonization of hydroxyl products to eventually form C=O bonds [17,18]. However, there remain some issues to be addressed in terms of C–H and C=C oxygenation reactions by CYPs, such as how to achieve highly selective hydroxylation, improve the conversion efficiency of epoxidation, and develop more CYPs to achieve ketonization. Using DNA recombination and protein engineering, the conversion rate, regioselectivity, and enantioselectivity of C–H and C=C oxygenation reactions catalyzed by CYPs can be significantly improved,

Peer review under responsibility of KeAi Communications Co., Ltd.
* Corresponding author.
E-mail address: weisong@jiangnan.edu.cn (W. Song).

https://doi.org/10.1016/j.synbio.2022.04.009
Received 23 March 2022; Received in revised form 24 April 2022; Accepted 26 April 2022
Available online 8 May 2022

which makes CYPs highly desirable for chemical synthesis.

In this review, we outline the recent advances and related applications in three types of C–H and C=C oxygenation reactions catalyzed by CYPs: hydroxylation, epoxidation, and ketonization. Based on published reviews, we further classify and summarize the strategies to improve the catalytic efficiency and selectivity of the above mentioned reactions, thus providing a reference for protein engineering approaches to specific problems. In addition, we summarize the synthetic applications of C–H and C=C oxygenation reactions catalyzed by CYPs and prospect the development of new functions of CYPs based on the latest research findings. Overall, this review comprehensively summarizes the current research and application of C–H and C=C oxygenation reactions catalyzed by CYPs and emphasizes the potential of CYPs. Undoubtedly, the P450 enzyme functional system provides a template and new insights for large-scale C–H and C=C oxygenation reactions.

1.1. Hydroxylation catalyzed by CYPs

Hydroxylation of the C–H bond is the most common catalytic reaction for CYPs, which rapidly activates inert molecules by introducing OH groups. However, the hydroxylation of alkene substrates generally has a low selectivity or an inability to introduce an oxygen atom into the desired position. In this section, taking representative aliphatic alkanes as examples, we describe the common issues, focusing on the relevant universal strategies to improve the selectivity of CYP-catalyzed hydroxylation reactions. Depending on the source of the oxygen atom, hydroxylation reactions can be classified as O_2- or H_2O_2-mediated [19,20].

1.1.1. O_2-mediated hydroxylation

The classic O_2-mediated two-electron oxygen transfer cycle is the main pathway of hydroxylation by CYPs. It begins with reducing the aqua-ferric resting state by accepting one electron owing to the entry of substrate molecules into the active site (Fig. 1) [21]. Subsequently, O_2 uptake leads to the ferrous state and reductive activation generating an oxyferrous intermediate. The addition of a second electron to the oxyferrous intermediate yields a peroxo-ferric derivative and forms a hydroperoxo-ferric intermediate (Cpd 0) via distal oxygen protonation [22]. Afterwards, the second proton is transferred to the distal OH group of Cpd 0, leading to O–O bond heterolysis and water release and the formation of an electrophilic π-cation radical oxoferryl state (Cpd I) [23,24]. The above mentioned conversion of Cpd 0 to Cpd I is referred to as the coupling-I pathway. Subsequently, Cpd I oxidizes the substrate by abstracting an H atom, which decides the placement of the OH group and regioselectivity, thereby generating the caged substrate radical coordinated to the iron hydroxo complex (Cpd 2) [23,25]. Finally, the substrate is replaced by a water ligand and recombines with the protonated oxygen bound to iron, thereby forming hydroxyl products.

The catalytic mechanism of hydroxylation and epoxidation catalyzed by CYPs is shown. Black lines represent the classic O_2-mediated two-electron oxygen transfer cycle, red dashed lines represent the hydrogen peroxide shunt bypass, gray lines represent the uncoupling pathway, and outer red dashed circles represent the involved intermediates in epoxidation different from those in hydroxylation.

According to the above mechanism, O_2-mediated regioselectivity is mainly controlled by the position of the H-atom extracted by Cpd I. However, for benzene, steroids, or chain fatty acids, multiple C–H bonds with the same extraction probability reduce hydroxylation regioselectivity. Specific C–H bonds can increase the possibility of H-atom extraction by shortening the distance from the active site, thus improving the regioselectivity of the specific position. This is usually achieved by adjusting the substrate-binding conformation [26,27].

The substrate-binding conformation at the active site is usually adjusted by systematically enlarging the substrate pocket, introducing new binding sites, and employing scanning chimeragenesis. A larger substrate pocket provides more space for substrate molecules to adjust the binding conformation, thus allowing specific C–H bonds to be closer to the heme and affecting regioselectivity and enantioselectivity [28]. This adjustment can be achieved by replacing the active site residues with smaller ones [29]. For example, Phe87 of CYP102A1 mutated into Ala turned the substrate terminal and the *pro-S* side of the C–H bond toward the heme, leading to a 24% increase in regioselectivity at

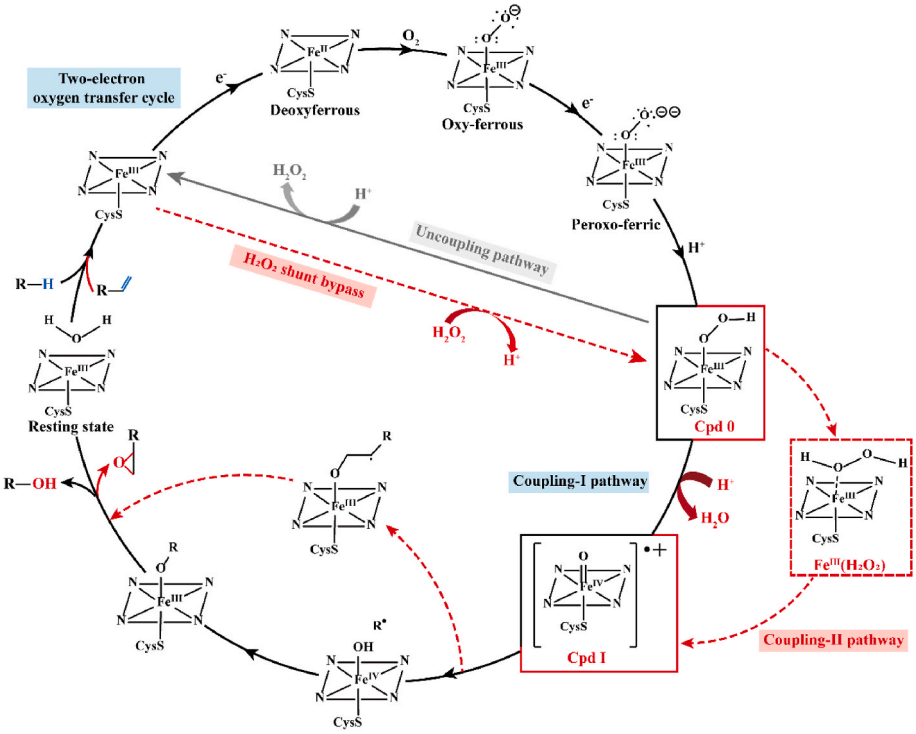

Fig. 1. Catalytic mechanism of CYPs.

position ω-5 [30]. Similarly, the L354I mutant in CYP153A33 provided approximately a 76% increase in ω-1 selectivity[31]. The V78A and I263G mutants in CYP102A1 and the G307A and S233G mutants in CYP153A33 enhanced regioselectivity for new positions that could not be catalyzed by the wild type [30,32]. In addition, introducing new binding sites can change the rigid binding conformation, which addresses the limitation of intrinsic binding anchors and acquires new polar anchors to attract different substrate groups closer to the heme [26]. For instance, the S72Y mutant in CYP102A1 increased the selectivity for position ω-9 by 9%28 whereas the M179Q mutant in CYP107Z14 increased the ratio of CsA-9-OH (γ-hydroxy-*N*-methyl-L-Leu^{9} -CsA) to CsA-4-OH up to 60%, compared with the wild-type (31%) [33]. The last strategy is the scanning chimeragenesis method [34]. By scanning the active site of highly selective CYPs, the residues near the binding substrate are transferred to the substrate recognition sites of other CYPs to form protein chimeras, thus improving their selectivity for specific substrates [35]. However, it is not widely used to adjust the substrate-binding conformations as it is often accompanied by damage to hydroxylation capacity [34]. The most representative example of scanning chimeragenesis is the fusion of CYP102A1 chimeras with the corresponding residues from CYP4C7, which showed 27% regioselectivity for position ω-6, where the wild-type showed difficulties in catalysis [36]. The details of the above examples were listed in Table 1.

In addition, the fusion of exogenous redox proteins to improve the enzymatic efficiency of hydroxylation, combined with adjustment of the substrate-binding conformation to regulate regioselectivity, is a common combination strategy for O_2-mediated hydroxylation with high efficiency and selectivity [44]. A representative example is the CYP105AS1 from *Amycolatopsis orientalis* fused to the RhF reductase of CYP116B1, which initially catalyzed the efficient hydroxylation of compactin to 6-epi-pravastatin. This fusion protein was further evolved to the P450(Prava) mutant to produce the pharmacologically effective pravastatin via changing the compactin binding modes and inverting its natural stereoselectivity [45]. The fusion of the diflavin reductase domain of CYP102A1 and the G307A mutant in CYP153A33 increased the conversion rate of C12 saturated fatty acids by 12%, and the yield was enhanced when the corresponding methyl ester was used as the substrate [31]. In fact, fusing exogenous redox proteins improves the catalytic efficiency of the whole cycle by reinforcing electron transport efficiency. The inefficient coupling of the electron transport system (Table 2) to P450 enzymes often becomes the rate-limiting step of the

Table 1
O_2-mediated hydroxylation catalyzed by CYPs.

Substrate	Variant	Conc. (mM)	Con. (%)	Enantiomeric excess (%)	References
Octanoic acid	CYP153A33	1	–	–	[31]
	CYP153A33 G307A variant	1	20.3	98.4(ω)	[31]
Nonanoic acid	CYP153A33	1	1.7	97.5(ω), 2.5(ω-1)	[31]
	CYP153A33 L354I variant	1	2	24.4(ω), 75.6(ω-1)	[31]
	CYP153A33 L354F variant	1	1.2	83 (ω), 17(ω-1)	[31]
	CYP153A33 G307A variant	1	26	98.9(ω), 1.1(ω-1)	[31]
Dodecanoic acid	CYP102A1	0.5	34	49(ω-1), 30(ω-2), 21(ω-3)	[37]
	CYP102A1 T268A variant	0.5	10	47(ω-1), 34(ω-2), 19(ω-3)	[37]
	CYP102A1 F87G variant	0.5	n.r.	19(ω-4), 34(ω-5)	[28]
	CYP102A1 F87V variant	0.5	n.r.	4(ω-4), 3(ω-5)	[28]
	CYP102A1 F87S variant	0.5	n.r.	16(ω-4), 7(ω-5)	[28]
	CYP102A1 F87A/V78A/I263G variant	0.5	54	8(ω-4), 23(ω-5), 4(ω-6), 14(ω-7), 2(ω-8), 3(ω-9)	[28]
	CYP102A1 F87A/S72Y/V78A variant	0.5	71	1(ω-4), 3(ω-5), 25(ω-6), 16(ω-7), 5(ω-8), 9(ω-9)	[28]
	CYP102A1-CYP4C7 chimera: 73–78	0.25	n.r.	26(ω-4), 9(ω-5), 27(ω-6)	[35]
	CYP153A33	0.2	64	97(ω)	[31]
	CYP153A33 G307A variant -CYP102A1 fusion protein	50	12	>95(ω)	[38]
	CYP153A33	0.28	25.6	ω-specific	[39]
	CYP153A33 P136A variant	0.23	60.9	ω-specific	[39]
	CYP102 Krac_9955	1	nr	6(ω-1), 16(ω-2), 72(ω-3)	[40]
Tridecanoic acid	CYP102A1	2	nr	19(ω-1), 64(ω-2), 17(ω-3)	[37,41]
Tetradecanoic acid	CYP153A33	1	48.4	97.1(ω)	[31]
	CYP153A33 G307A variant	1	68.6	96.8(ω)	[31]
	CYP102A1	0.5	88	48(ω-1), 27(ω-2), 25(ω-3)	[37]
	CYP505A30	1	nr	63(ω-1), 28(ω-2), 9(ω-3)	[42]
Pentadecanoic acid	CYP102A1	0.5	88	36(ω-1), 43(ω-2), 21(ω-3)	[37]
12-Methylmyristic acid	CYP102A1	0.5	90	85(ω-1), 2(ω-2), 13(ω-3)	[43]
13-Methylmyristic acid	CYP102A1	0.5	76	15(ω-1), 83(ω-2), 2(ω-3)	[43]
Hexadecenoic acid	CYP102A1	0.5	93	23(ω-1), 43(ω-2), 34(ω-3)	[37]
	CYP102A1 T268A variant	0.5	21	25(ω-1), 42(ω-2), 33(ω-3)	[37]
	CYP102A1-CYP4C7 chimera: 73–78	0.2	n.r.	7(ω-4),10(ω-5), 27(ω-6)	[34]
	CYP102A1-CYP4C7 chimera: 78–82	0.2	n.r.	8(ω-4),4(ω-5), 4(ω-6)	[34]
14-Methylpalmitic acid	CYP102A1	0.5	87	85(ω-1), 2(ω-2), 13(ω-3)	[43]
15-Methylpalmitic acid	CYP102A1	0.5	96	9(ω-1), 89(ω-2), 2(ω-3)	[43]

Table 2
Electron transport system of CYPs [53,54].

Classification	Electron transport chain	Redox partners	Sources
Class I	NADH → FdR → Fdx → heme	Ferredoxin reductase (FdR, FAD), Ferredoxin (Fdx, [2Fe–2S] cluster)	*Bacterial* or *Mitochondrial*
Class II	NADPH → CPR → heme	Cytochrome P450 reductase (CPR), consisting of FMN and FAD	*Bacterial* or *Mitochondrial*
Class III	NAD(P)H → FdR → Fld → heme	Ferredoxin reductase (FdR, FAD), FMN-containing flavodoxin (Fld)	*Bacterial*
Class IV	Pyruvate/CoA → OFOR → Fdx → heme	2-Oxoacid: ferredoxin oxidoreductase (OFOR)	*Bacterial*
Class V	NADPH → FdR → Fdx-heme	Ferredoxin reductase (FdR, FAD), Ferredoxin (Fdx)	*Bacterial*
Class VI	NAD(P)H → FdR → Fld-heme	Ferredoxin reductase (FdR, FAD), FMN-containing flavodoxin (Fld)	*Bacterial*
Class VII	NAD(P)H → PFOR-heme	Phthalate-family oxygenase reductase (PFOR), consisting of FMN and Fdx ([2Fe–2S] cluster)	*Bacterial*
Class VIII	NAD(P)H → BMP-heme	BMP consisting of ferredoxin reductase (FdR, FAD) and FMN	*Bacterial*
Class IX	NADH → heme	–	*Bacterial*
Class X	HEME	–	*Plant* or *Mammal*

entire reaction [46]. This fusion can be achieved by linking the P450 enzyme domain and the redox system into a chimera using DNA recombination technology through simple residues (linker), thereby forming a polypeptide protein to address inefficient coupling [47,48]. For example, the RhFRED reductase domain of P450RhF from *Rhodococcus* sp was fused to P450Pikc to form a novel self-sufficient chimera with an efficient electron transport system, resulting in a fourfold increase in hydroxylation activity for both YC-17 and narbomycin [49,50]. Furthermore, the length, hydrophobicity, and the secondary structure of the linker affect the expression, coupling efficiency, and correct folding of the fusion protein. For example, in the construction of the fusion proteins of CinA and CinC of P450cin, co-expression activity was the highest when the length of the linker was 10 residues [51]. CYP102A1 reductase (BMR) was fused to the *N*-terminally modified P450 3A4 via a glycine hinge to construct the self-sufficient chimeric 3A4-BMR. Compared with 3A4-3GLY-BMR, 3A4-5GLY-BMR demonstrated a 1.26-fold increase in coupling efficiency of testosterone hydroxylation [52].

1.1.2. H_2O_2-mediated hydroxylation

Unlike O_2-mediated hydroxylation, H_2O_2-mediated hydroxylation takes hydrogen peroxide as the sole oxygen atom source and electron donor without complex electron transport systems; therefore, only the heme domain is required [54]. Only a few peroxygenases can catalyze H_2O_2-mediated hydroxylation, do not require cofactors and redox protein partners, and generally show high regioselectivity or enantioselectivity [55]. Peroxygenases can directly convert the resting state into Cpd 0 by virtue of electrons contributed by H_2O_2, avoiding the complicated electron transport process [19]. Subsequently, H_2O_2 provides a proton to the proximal oxygen of Cpd 0, resulting in the formation of $Fe^{III}(O_2H_2)$ intermediates as a transient second oxidant, followed by O–O homolysis and release of OH radicals [56]. Finally, the hydrogen bond network locks the hydroxyl radical and forces it to extract a proton from the iron complex, thereby generating Cpd I to hydroxylate substrates with high selectivity [57]. The Cpd 0 → $Fe^{III}(O_2H_2)$ → Cpd I process is referred to as the coupling-II pathway, and the abbreviated cycle using H_2O_2 is called hydrogen peroxide shunt bypass (Fig. 1) [23].

H_2O_2-mediated hydroxylation using the coupling-II pathway generally shows higher regioselectivity than the coupling-I pathway, which may also be due to the strict substrate-binding pocket of peroxygenases [56]. For example, CYP152B1 catalyzes the production of (*S*)-2-hydroxymyristic acid from the natural substrate myristic acid with 94% enantiomeric excess (ee) [58]. However, hydroxylation mediated by H_2O_2 is often accompanied by oxidative decarboxylation (Table 3), so the regulation of reaction selectivity cannot be ignored. Thus far, the mechanism of oxidative decarboxylation as a side reaction catalyzed by CYPs remains controversial. The most convincing explanation is that oxygen rebound causes substrate hydroxylation or that a carbocation triggers decarboxylation after a hydrogen atom is extracted from the α- or β-position of the substrate to obtain the corresponding carbon radical [59,60].

Reaction selectivity is influenced by the specific substrate molecules with different carbon chain lengths and can be efficiently controlled by adjusting substrate binding via mutations in the conserved binding site [61]. The most common adjustments include mutations of conserved arginine as a binding anchor to the carboxyl-terminal of the substrate [62,63]. For example, when the substrate was a C10 saturated fatty acid, the R245L mutant of CYP152L1(OleT_{JE}) increased the conversion rate of α-hydroxylation by 78% and decreased decarboxylation from 51% to 0.1%, whereas the R245E mutant completely lost hydroxylation activity. However, the R254L mutant showed significant decreases of 48% and 97% in hydroxylation activity for C12 and C14 saturated fatty acids, respectively [60]. The affinity of CYP152L1 for substrates decreases as the chain length of fatty acids increases [64]. In summary, a series of conserved arginine mutants influence the proton extraction process of the substrate by changing the binding conformation and controlling reaction selectivity.

1.2. Epoxidation catalyzed by CYPs

CYPs also catalyze the epoxidation of C=C bonds to form oxirane-containing chemicals. As a typical carbon-oxygen cyclization reaction, epoxidation involves non-rotatable unsaturated bonds and ring tension, unlike hydroxylation. In this section, we focus on the central questions of epoxidation, namely the relevant strategies for improvement of catalytic efficiency. According to the source of oxygen atoms, epoxidation reactions can be classified as O_2- or H_2O_2-mediated epoxidation.

1.2.1. O_2-mediated epoxidation

In the presence of O_2, epoxidation and hydroxylation are often

Table 3
Two reactions catalyzed by CYP152 peroxygenases (C12 fatty acids) [19].

Substrate[a]	Enzyme	Product distribution (%)		
		Hydroxylation	Decarboxylation	Undecanal formation[b]
Dodecanoic acid	CYP152A1	72.5%	12.5%	15%
	CYP152B1	94.6%	n.r.	5.4%
	CYP152L1	27.1%	63.6%	9.3%
cis-2-dodecenoic acid	CYP152A1	3.2%[c]	n.r.	56.5%
	CYP152B1	n.r.[c]	n.r.	63.2%
	CYP152L1	89.3%[c]	n.r.	1.8%
trans-2-dodecenoic acid	CYP152A1	3.3%[c]	n.r.	58.2%
	CYP152B1	n.r.[c]	n.r.	62.4%
	CYP152L1	98.5%	n.r.	1.5%

[a] Reactions conditions: 0.5 mM substrate; 0.001 mM CYP152 enzyme; 0.5 mM alditol oxidase (AldO) and 10% glycerol for in situ generation of H_2O_2 as the oxygen source; 30 °C; 6 h.
[b] Undecanal formation is the sequential hydroxylation, isomerization, and decarboxylation.
[c] Other oxygenation reactions were detected, including epoxidation and ketonization.

observed simultaneously in olefin oxygenation catalyzed by CYPs, causing an increase in the cost of product purification and separation. For example, CYP102A1 showed a low selectivity for catalyzing α-isophorone oxygenation, where hydroxyl products and epoxides were found [65]. CYP MycG catalyzed the biosynthesis of mycinamicin II (M-II) from mycinamicin IV (M-IV), where 20.6% of M-IV underwent epoxidation to mycinamicin-I and 77.4% underwent sequential hydroxylation and epoxidation to M-II [66]. In fact, the mechanism of epoxidation was reported to generate a metal-carbon radical intermediate instead of Cpd 2 intermediate in hydroxylation (Fig. 1) [67,68].

To achieve specific O_2-mediated epoxidation, the coupling-II pathway has been artificially constructed by interrupting the protonation process mediated by acid-alcohol pairs. Once the normal proton transfer through acid-alcohol pairs is interrupted, direct conversion from Cpd 0 to Cpd I is impeded, and the electrons transported by redox systems reduce O_2 to H_2O_2, which induces the formation of the $Fe^{III}(O_2H_2)$ transient intermediate [23,69]. Nucleophilic attacks from the generated Cpd I intermediate to olefin results in the formation of an iron-alkoxy radical complex intermediate, and epoxides are finally released [70]. Collectively, disruption of the acid-alcohol pairs terminates the coupling-I pathway and initiates the coupling-II pathway in the classic two-electron oxygen transfer cycle.

The disruption of acid-alcohol pairs can be achieved by mutation of the conserved threonine, which participates in Cpd 0 protonation. The alanine mutation eliminates the OH group and leaves no other electrically charged groups to transfer protons. The most typical example is the T252A mutant of CYP101A1 from *Pseudomonas putida* that specifically catalyzes the epoxidation of 5-methylenylcamphor but is associated with a lost capacity for effective hydroxylation. In contrast, the wild-type mainly catalyzed camphor hydroxylation [23]. This was the earliest evidence for the existence of the $Fe^{III}(O_2H_2)$ intermediate; however, the catalytic activity of the T252A mutant was decreased by 80% [69]. This change in catalytic efficiency may be explained by the increase in uncoupling efficiency due to the generation of hydrogen peroxide. This can be demonstrated by a study of the epoxidation of 4-vinylbenzoic acid catalyzed by CYP199A4 and its T252A mutant. CYP199A4 T252A mutant showed a 1.6-fold increase in NADH oxidation rate but a 40% decrease in coupling efficiency, resulting in reduced epoxidation efficiency [71,72].

Owing to the presence of electron transport systems in classic cycle, the fusion of exogenous redox proteins to achieve a more efficient electron transport process is suitable for improving O_2-mediated epoxidation activity (see section *O_2-mediated hydroxylation* above). For example, the epoxidation of epothilone C + D catalyzed by CYP167A1 (EpoK) co-expressed with Fdx_0135, a hybrid [3Fe–4S]/[4Fe–4S] ferredoxin from *Schlegelella brevitalea* DSM 7029, had a 90.93% conversion rate, which was 1.5-fold higher than that by single EpoK; in contrast, the conversion rate of epothilone C reached 100% in whole-cell transformation where EpoK was co-expressed with Fdx_A6445 (a similar ferredoxin to Fdx_0135) (Fig. 2b) [73]. In addition to the type of exogenous proteins, the interaction between exogenous proteins and CYPs can influence enzyme activity and reaction type. For example, the CYP MycG-RhFRED fused protein showed a 2.4-fold increase in the yield of oxidized product (mycinamicins I, II, and IV) compared with CYP MycG cooperated with separated RhFRED protein; however, the new *N*-demethylation of mycinamicins IV was observed during separation (Fig. 2a) [74].

The exogenous protein has relatively less influence on self-sufficient CYPs that do not require additional redox proteins. In this case, catalytic efficiency and selectivity are mainly controlled by the substrate-binding orientation, which is influenced and regulated by residues at the active site. For instance, the CYP102A1 F87V mutant achieved 99% 14(*S*)-15(*R*)-epoxidation in arachidonic acid, whereas the wild type yielded 20% epoxidation and 80% 18(*R*)-hydroxylation [75]. For the epoxidation of 1-hexene catalyzed by CYP102A1, the SH-44 mutant had 88% (*S*)-selectivity, the RH-47 mutant had 93% (*R*)-selectivity, and the wild type had 10% (*R*)-selectivity. The epoxidation activities of the SH-44 mutant (containing F87V and I263A) and RH-47 mutant (containing I263A, A82F, and A328V) were increased by 54.5- and 30.5-fold, respectively, compared to that of wild type [76]. Substitutions in key residues closest to the heme affect the oxygenation reactions catalyzed by CYPs and the selectivity and efficiency of other reactions (for example, asymmetric amination [77] and aminohydroxylation [78]).

In particular, the modification of the heme-propionate side chains, including the introduction of hydrophobic moieties or flavin moieties, is an emerging approach to optimize the performance of heme proteins

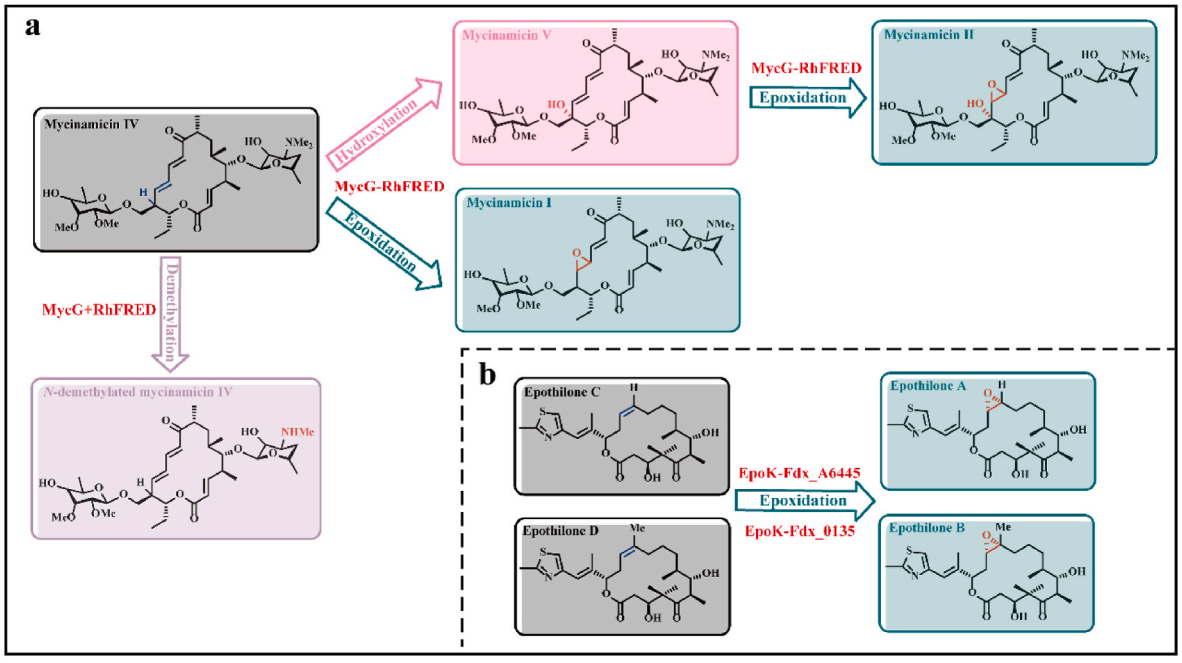

Fig. 2. Exogenous redox proteins for O_2-mediated epoxidation **a.** The biotransformation from mycinamicin IV catalyzed by CYP MycG with RhFRED protein; **b.** The biotransformation from epothilone C + D catalyzed by EpoK with Fdx proteins.

[79,80]. The heme-propionate side chains mediate the first protonation in the classic O_2-mediated two-electron oxygen transfer cycle, facilitating the synthesis of the Cpd 0 intermediate through the hydrogen bond network of the water chain [22]. Unlike relatively matured acid-alcohol pairs strategies that regulate the second protonation, the strategies targeting the heme-propionate side chains of CYPs are still under development. However, they have shown great potential in other heme-containing enzymes. This method helped achieve optimal results in myoglobins containing heme catalytic centers. For example, introducing the benzene group as a hydrophobic substrate-binding site into propionate side chains improved the catalytic efficiency ($Kcat/K_M$) of reconstituted myoglobin by 14 times [81]. Moreover, acidic substrates often lead to a lower CYP catalytic activity due to the disruption of the salt bridge or the hydrogen bond between the heme-propionate and the basic residue [82,83].

1.2.2. H_2O_2-mediated epoxidation

H_2O_2-mediated epoxidation utilizes the hydrogen peroxide shunt bypass to achieve a highly selective C–O cyclization reaction via the coupling-II pathway. There is a demand to prevent H_2O_2 escape; otherwise, H_2O_2 will degrade the unstable $Fe^{III}(O_2H_2)$ intermediate into a resting state, causing ineffective catalysis. This process, accompanied by the release of H_2O_2, is called the uncoupling pathway [23,84]. The much lower utilization rate of H_2O_2 than that of O_2 results in low efficiency of the coupling-II pathway in the hydrogen peroxide shunt bypass. Promoting the binding of free H_2O_2 near the active center to the heme and preventing the degradation of $Fe^{III}(O_2H_2)$ to release bound H_2O_2 are effective strategies to improve the H_2O_2 utilization rate [85]. Acid-alcohol pairs mediating the proton transfer process are critical for transforming Cpd 0 to Cpd I, thus significantly influencing the efficiency of the coupling-II pathway [70]. Based on the above, the conversion rate of H_2O_2-mediated epoxidation can be improved by (i) promoting H_2O_2 binding, (ii) enhancing the stability of the $Fe^{III}(O_2H_2)$ intermediate, and (iii) enhancing proton transfer efficiency.

Promoting the binding of H_2O_2 to the heme improves substrate efficiency in obtaining oxygen atoms during epoxidation and can be achieved by reconstructing the substrate pocket. Mutating small residues in the substrate pocket into amino acids with large side chains can prevent the escape of H_2O_2 molecules near the active site to some extent; thus, more H_2O_2 molecules can combine with the heme to catalyze the epoxidation of the substrate. An evident example is a series of variants in the 245th alanine of CYP152B1. Compared with the wild-type, which cannot catalyze styrene epoxidation utilizing H_2O_2, the A245D mutant successfully catalyzed this reaction, achieving a catalytic activity (k_{cat}) of 72 min^{-1} and a catalytic efficiency (k_{cat}/K_M) of 14 $M^{-1}s^{-1}$. In contrast, the A245E mutant achieved a k_{cat} and k_{cat}/K_M up to 280 min^{-1} and 190 $M^{-1}s^{-1}$, respectively [86]. Notably, the above substitution is usually not targeted at the gated residues for fear of hindering the substrate molecules into the active site and adjusting the binding conformation.

Enhancing $Fe^{III}(O_2H_2)$ stability is another effective strategy to enhance the utilization of H_2O_2 by CYPs. Unstable $Fe^{III}(O_2H_2)$ intermediates release the bound H_2O_2, switching the catalytic pathway from the coupling-II pathway to the uncoupling pathway, resulting in ineffective catalysis. The formation of $Fe^{III}(O_2H_2)$ is controlled by the positively charged residues in the acid-alcohol pairs, such as Asp251 in CYP101A1 [87]. Only when the basic residue is deprotonated its carboxylate side chain is rotated upward to form a hydrophobic salt bridge with other residues, thereby breaking the hydrogen bond between H_2O_2 and the water chain to facilitate the generation of the $Fe^{III}(O_2H_2)$ intermediate [22,88]. The stability of the $Fe^{III}(O_2H_2)$ intermediate can be enhanced by hydrogen bond interactions of polar residues [89]. The shorter the hydrogen bond provided by the residues, the more efficient the conversion of $Fe^{III}(O_2H_2)$ to Cpd I. A representative example is the methionine mutation Thr213 in CYP119. The T213M mutant formed a hydrogen bond between the sulfoxide oxygen of methionine-sulfoxide and the distal H of $Fe^{III}(O_2H_2)$, resulting in a 1.33- and 1.5-fold increase in the conversion rate and the ee value, respectively, when the substrate was *cis-b*-methyl styrene [90].

In addition to controlling the formation of $Fe^{III}(O_2H_2)$, acid-alcohol pairs are mainly responsible for proton transfer to promote the generation of Cpd I. Artificial construction of more efficient acid-alcohol pairs can enhance proton transfer efficiency and accelerate Cpd I generation, further improving H_2O_2-mediated epoxidation activity [70,72]. For example, the T268E mutant of CYP102A1 acquired oxygenation activity depending on H_2O_2. The T213E mutant of CYP119 showed a tenfold increase in epoxidation activity compared to the wild-type [14,86]. Compared to the conserved threonine as a non-ionizing polar amino acid, glutamate carries negative charges and thus shifts the protonation/deprotonation state more flexibly, speeding up the proton transfer of the acid-alcohol pair channel (Fig. 3). In addition, dummy molecules with carboxyl and imidazolyl groups can be inserted into CYPs as alternative acid-alcohol residues, shifting the enzyme state from the resting low-spin to the active high-spin [91,92]. For instance, the addition of the dual functioning molecule N-(ω-imidazolyl)-hexanoyl-L-phenylalanine (Im-C6-Phe) to the F87A mutant of CYP102A1 resulted in a 30-fold improvement in the total turnover number (TON) for epoxidation [93].

1.3. Ketonization catalyzed by CYPs

In addition to hydroxylation and epoxidation, ketonization is also an oxidation reaction of C–H bonds catalyzed by CYPs. However, there are very few cases of ketonization; therefore, this chapter will take representative ketonization catalyzed by CYPs to introduce the ketonization mechanism. In contrast to the one-step catalysis of hydroxylation and epoxidation, the ketonization of methylene is a two-step reaction, and it is only mediated by O_2 [18,94]. Using the classic two-electron oxygen transfer cycle, rare CYPs continuously introduce two hydroxyl groups to the same carbon atom of substrate molecules, followed by spontaneous dehydration to form ketones. First, CYPs hydroxylate substrate molecules to obtain intermediates. Subsequently, the same CYPs catalyze the C atom with a hydroxyl group in substrate molecules ketonization to obtain final ketone products. In the early stage of the reaction, two successive steps result in the conversion of all initial substrate molecules to ketones. However, the accumulation of hydroxyl by-products usually far exceeds that of ketones in the middle and late stages of the reaction [18]. Therefore, the ketonization catalyzed by CYPs is usually inefficient, and this phenomenon may be explained by the ketonization catalyzed by *Sa*AcmM (Fig. 4a).

Oxidizing a secondary alcohol group is the proven mechanism of *Sa*AcmM to catalyze ketonization, while the catalytic mechanism of other CYPs with similar functions has not been clearly elucidated. The uncoupling relationship between hydroxylation and ketonization is mainly caused by feedback inhibition of ketone products, but it has no parallel effect on the hydroxylation reaction. The spatial difference between the two reactions results in the accumulation of hydroxyl products and the formation of a small number of ketones [18]. This feedback inhibition can be relieved by separating the final products from the system in time or gene engineering to remove the final product inhibition.

So far, only a few CYPs catalyzing ketonization have been discovered, among which the most well-known are *Sa*AcmM and CYP107Z12 (Ema). *Sa*AcmM from *Streptomyces antibioticus* is a new family of peptidylproline-ketonizing CYPs and catalyzes proline hydroxylation and ketonization in the actinomycin precursor [95]. CYP107Z12 (Ema) from *Streptomyces hygroscopicus* catalyzes the conversion of avermectin B1 to its hydroxyl and ketone derivatives (Fig. 4b) [96]. Thus far, there have been few reports on ketonization catalyzed by CYPs, and related protein engineering strategies need to be further developed.

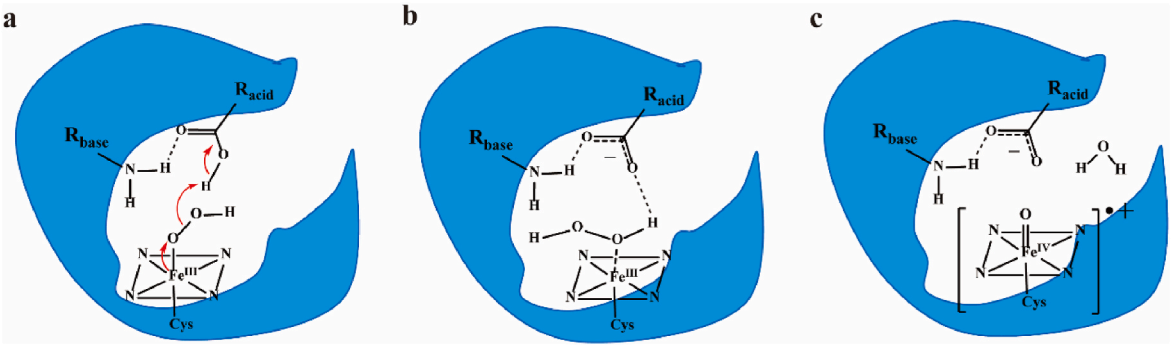

Fig. 3. Artificial acid-alcohol pairs in the active site of CYPs **a.** Common principle of the Cpd 0 in the presence of acid-alcohol catalytic residues in CYPs; **b.** Common principle of the $Fe^{III}(O_2H_2)$ intermediates in the presence of acid-alcohol catalytic residues in CYPs; **c.** Common principle of the Cpd I in the presence of acid-alcohol catalytic residues in CYPs. The carboxylate group comes from a glutamic acid residue. The amino group derives from a histidine or an arginine residue, whose N–H bond stabilizes the negative charge of the acid-base pair.

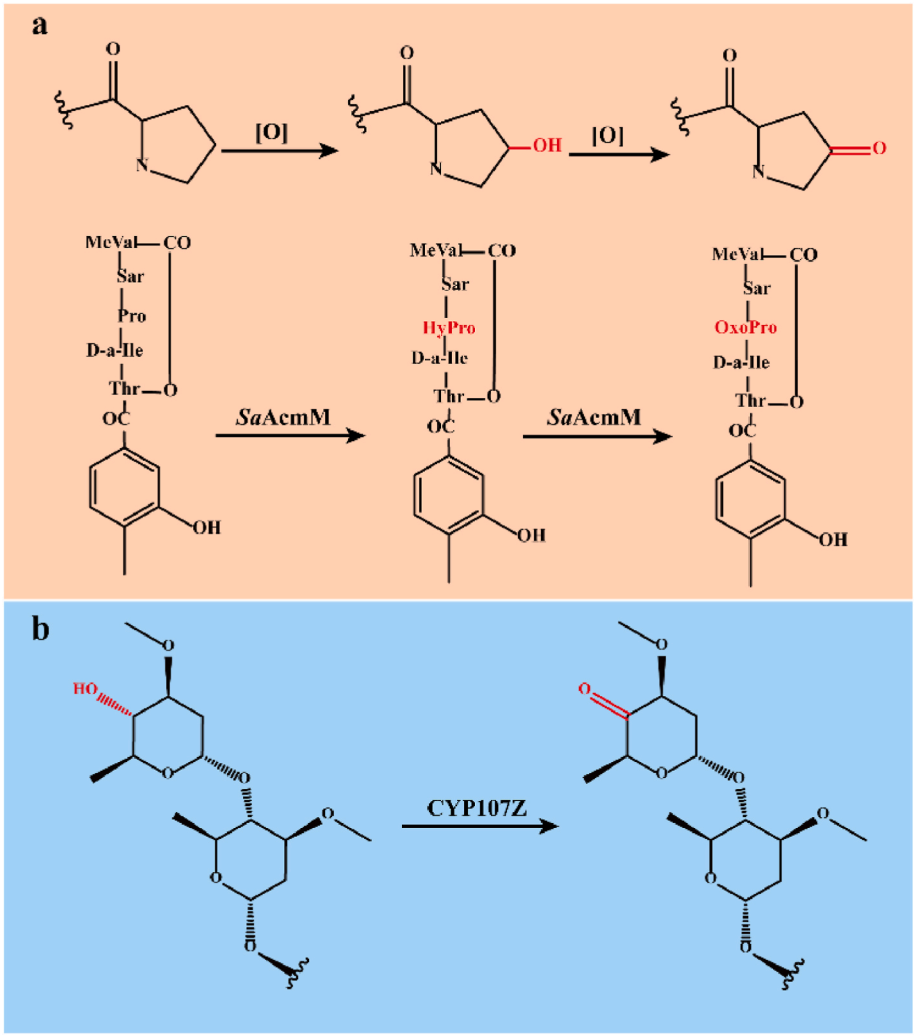

Fig. 4. The ketonization reactions catalyzed by CYP107Z family and *Sa*AcmM **a.** The conversion of actinomycin to 4-oxoproline-actinomycin catalyzed by *Sa*AcmM. **b.** The conversion of avermectin B1 to 4″-oxo-avermectin B1 catalyzed by CYP107Z. Abbreviations: Sar, sarcosine; MeVal, *N*-methyl-L-valine.

1.4. Applications of C–H and C=C oxygenation reactions

Among the three types of C–H and C=C oxygenation reactions catalyzed by CYPs, hydroxylation and epoxidation are more widely used in practical applications. The direct introduction of C–O bonds provides a potent method for synthesizing complex compounds and pharmaceutical intermediates, thus increasing the value of cheap raw materials [97–99].

1.4.1. Biosynthesis with CYPs catalyzed C–H and C=C oxygenation

As an early focus of CYP whole-cell catalysts, hydroxylation has been partially and commercially applied, especially in drug synthesis. High-

selectivity hydroxylation catalyzed by CYPs plays a vital role in synthesizing antibiotics and sterol derivatives. For example, an engineered CYP102A1 mutant was applied to the enantioselective total synthesis of norditerpenoid alkaloid nigelladine A. This catalyzes highly selective hydroxylation of the allylic C–H bond in the presence of three other oxidizable sites, eventually resulting in 43% yield based on redesigned biocatalytic process (Fig. 5a) [100]. The CYP105AS1 mutants from *Amycolatopsis orientalis* synthesized pravastatin from compactin and completely reversed wild-type stereoselectivity, resulting in pravastatin to 6-epi-pravastatin ratio changing from 3:97 to 96:4 (Fig. 5b) [44,45]. CYP_{lun} from *Curvularia lunata* converted androstenedione and cortexolone to 14α-OH-androstenedione (60% w/w yield and regioselectivity up to 99%) and 14α-OH-cortexolone (26% w/w yield and regioselectivity up to 40%), respectively (Fig. 5c) [101]. During the biosynthesis of paclitaxel, half of the enzymatic reactions were catalyzed by CYPs. The CYP725A family played a significant role [102], such as the oxygenation of taxadiene catalyzed by CYP725A4 and the titer of T5α-ol-taxadiene reached 78 mg/L and 570 mg/L in *Saccharomyces cerevisiae* [103] and *E. coli* [104], respectively. Furthermore, various CYP102A1 mutants produced almost all mammalian metabolites of verapamil and astemizole through hydroxylation, with 78% highest total conversion rate and ≥75% selectivity (Fig. 5d–e) [105]. In fact, hydroxylation catalyzed by CYPs is usually the first step in activating the starting molecules in multi-enzyme cascades [97,99]. For example, a mature cascade consisting of a highly selective CYP102A1 variant and alcohol dehydrogenase (ADH) from *Lactobacillus kefiri* transformed cyclohexane to any stereoisomer of cyclohexane-1,2-diol, up to 92%–98% ee and 80%–93% de (Fig. 5f) [106]. Based on the CYP-ADH cascade, the complement of Bayer–Villiger monooxygenase can produce lactones, such as 2-oxocanone and ε-caprolactone [107]. Furthermore, the combination of tyrosine phenol lyase with the CYP102A1 variant catalyzed asymmetric amination starting from mono-substituted benzenes and resulting in 5.2 g/L L-DOPA surrogates [108].

Both hydroxylation and epoxidation can use alkenes and other cheap and readily available starting materials to obtain high added-value products. For instance, a series of terminal alkenes were converted to the corresponding (*S*)- or (*R*)-epoxides using engineered CYP102A1 mutants, with epoxidation turnovers up to 1370, catalytic selectivity up to 95%, and enantioselectivity up to 83% ee (Fig. 6a) [109]. In addition, CYP isoforms consisting of 2E1, 1A2, and 3A4 converted 4,5-benzoxepin to 2,3-epoxyoxepin; this is a reactive intermediate that rapidly undergoes ring-opening and isomerization to form 1*H*-2-benzopyran-1-carboxaldehyde, which is the primary method for benzene to open the ring and obtain muconaldehyde (Fig. 6b) [110]. A P450pyr triple mutant efficiently catalyzed (*R*)-selective epoxidation of *para*-substituted styrenes, resulting in 82%–97% conversion rate and 98.5%–

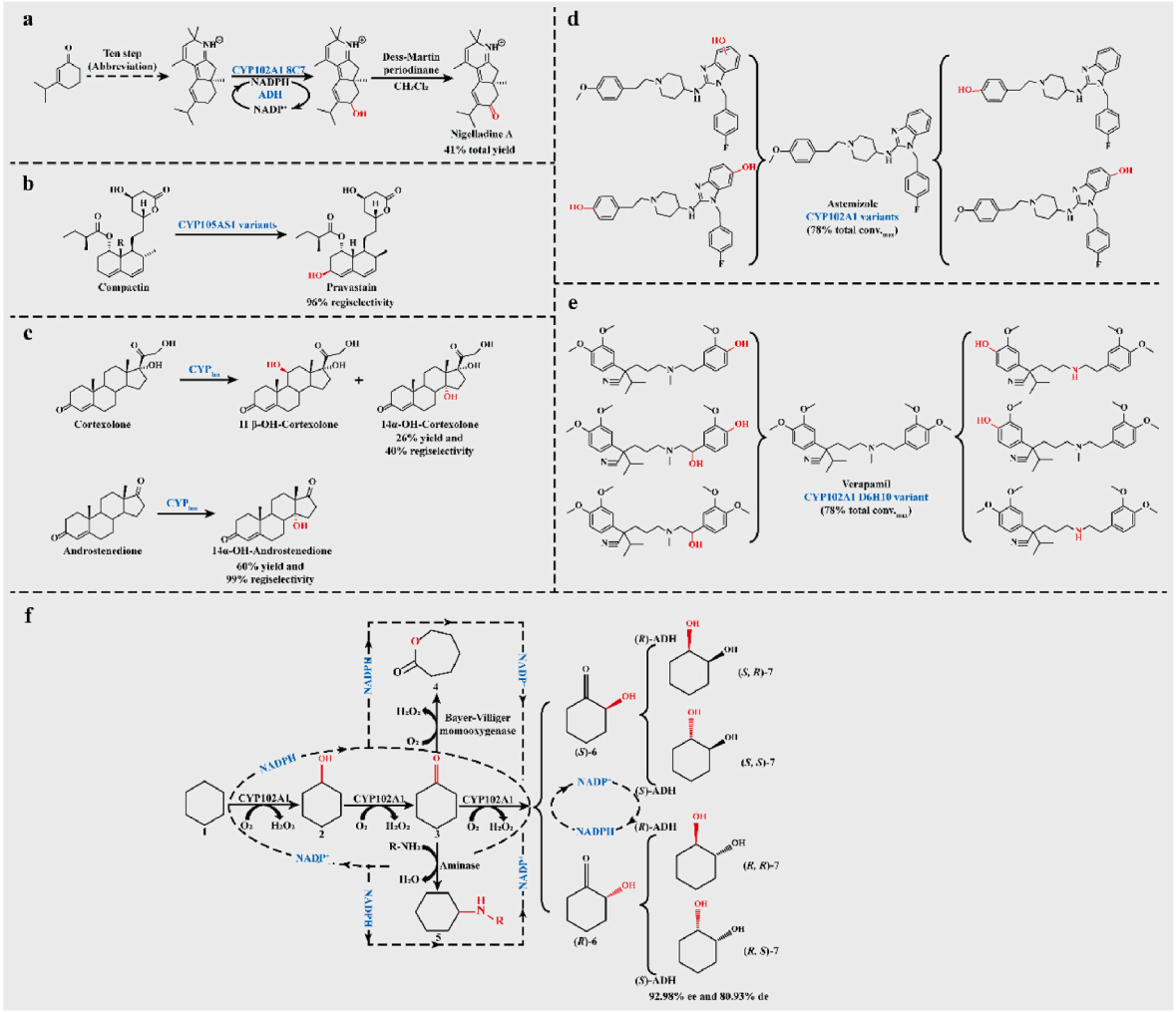

Fig. 5. Hydroxylation reactions catalyzed by CYPs in production **a.** Starting from 3-isopropyl-2-cyclohexenone to produce nigelladine A; **b.** Synthesizing pravastatin from compactin; **c.** Introducing a hydroxyl group into androstenedione and cortexolone to produce 14α-OH-androstenedione and 14α-OH-cortexolone respectively; **d.** Converting astemizole to mammalian metabolites; **e.** Converting verapamil to mammalian metabolites; **f.** Three types of representative multi-enzyme cascades involving O_2-mediated hydroxylation and ketonization catalyzed by CYP102A1. ADH, alcohol dehydrogenase.

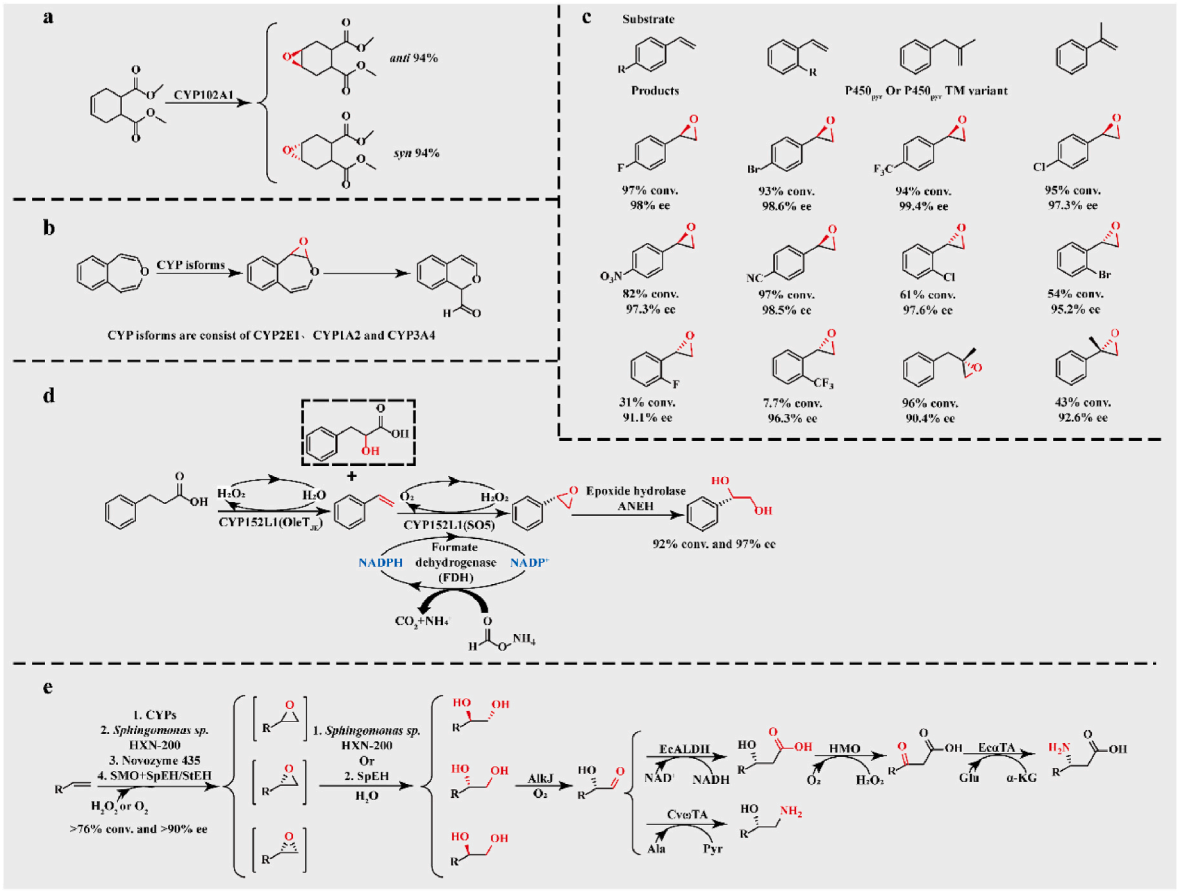

Fig. 6. Epoxidation reactions catalyzed by CYPs in production **a.** The diastereoselective epoxidation of dimethyl *cis*-1,2,3,6-tetrahydrophthalate catalyzed by CYP102A1; **b.** Converting 4,5-benzoxepin to 2,3-epoxyoxepin via CYP isoforms; **c.** A series of epoxidation of substituted styrenes catalyzed by $P450_{pyr}$ variant; **d.** The two-step oxidative cascade catalyzed by $OleT_{JE}$ and CYP102A1; **e.** A general model for multi-enzyme cascades involving CYPs-catalyzed epoxidation.

99.5% ee (Fig. 6c) [111]. The generated (*R*)-*para*-substituted styrene oxides are important pharmaceutical intermediates that are hardly produced by other chemical or enzymatic systems. A novel P450tol from *Rhodococcus coprophilus* co-expressed with glucose dehydrogenase converted *meta*- and two *ortho*-substituted styrenes to their corresponding (*R*)- oxides, with 74%–99% conversion rate and 92%–99% ee [112]. In the multi-enzyme cascades, CYP-catalyzed epoxidation first introduces oxirane, followed by hydrolases, such as epoxidase from glycol, to the substrate molecules through ring-opening reactions, realizing the introduction of two oxygen atoms to adjacent C atoms in the substrate molecules. For instance, the biocatalytic cascade consisting of P450 $OleT_{JE}$, CYP102A1(SO5), and epoxide hydrolase ANEH converted 3-phenyl propionic acid to (*R*)-phenyl glycol, resulting in 97% ee and a conversion rate of up to 92% (Fig. 6d) [113]. $OleT_{JE}$ first decarboxylated the starting substrate to styrene, which was converted to (*R*)-styrene oxide by CYP102A1 (SO5) with high (*R*)-selectivity, followed by an ANEH-catalyzed ring-opening reaction to obtain (*R*)-phenyl glycol. For *ortho*- or *meta*-substituted 3-phenyl propionic acid derivatives, the above cascades usually led to a conversion rate of >76% and ee of >90%. The multi-enzyme cascade, epoxidation, and ring-opening have been widely used in various organic syntheses with high selectivities, such as the asymmetric synthesis of vicinal diols, 1,2-amino alcohols, α-hydroxy acids, and α-amino acids from alkenes (Fig. 6e) [114].

1.4.2. Heterologous expression of CYPs for biosynthesis

In practical application, CYPs whole-cell biocatalyst is the major form because of the stability of active components and the cofactors provided by hosts [115]. Therefore, improving the heterologous expression of CYPs for whole-cell transformation is crucial for the biosynthesis of various products. These strategies can be divided into environmental, molecular, and gene levels.

Environmental level optimization is the selection of a heterologous host, which influences gene transcription, translation, and protein modification. *E. coli* BL21(DE3) is the most common prokaryotic host and is applied to the most bacterial CYPs [116]. In contrast, yeast is generally used to express the membrane-bound CYPs, such as *Saccharomyces cerevisiae* [117] and *Pichia pastoris* [118], *Yarrowia lipolytica* [119], *Schizosaccharomyces pombe* [120], and *Arxula adeninivorans* [121] have been used as eukaryotic hosts, and their ability to modify CYPs have been studied. For example, the expression of CYP88D6 and CYP72A154 in *S. cerevisiae* [122] and that of CYP57B3 in *P. pastoris* [123] were examined.

Co-expression with protein partners and supplementation of the prosthetic group improve the expression of CYPs at the molecular level. The representative protein partners are CPRs and GroES/GroEL. For example, PPDS from *Panax ginseng* fused to CPR-ATR1 via a GSTSSGSC polypeptide linker lead to a 4.5-fold increase in catalytic activity [124]. Unlike the CPRs used widely in yeast hosts, GroES/GroEL is generally applied to the expression of CYPs in *E. coli.* CYP79A2 from *Arabidopsis thaliana* co-expressed with the heat shock protein GroES/GroEL resulted in a 4.6-fold increase in catalytic activity for *E, Z*-phenylacetaldoxime [125]. Supplementing a moderate prosthetic group can enhance the expression of CYPs in microbial hosts, most of which lack the pathway to generate heme [126]. The addition of heme (FePPIX) or 5-aminolevulinic acid (ALA) is a common strategy and ALA has better effects than FePPIX owing to the absence of an uptake system for FePPIX in the microorganism. For example, the supplementation of 0.5 mM ALA improved the activity of CYP153A33, raising the titer of 1,

12-dodecanediol produced from 0.26 mM to 0.58 mM [127]. Purified membrane human CYPs (CYP3A4, CYP21A2, and CYP17A1) were obtained at a 50–100 nmol yield via exogenous FePPIX supplementation combined with the introduction of the uptake genes [128].

Strategies at the gene level include codon optimization, *N*-terminal modification and endoplasmic reticulum (ER) engineering. Preferential codons for heterologous hosts increased the translation of inserted genes and improved the soluble expression of CYPs [129]. For example, the catalytic activity of integrated CYP176A1 for hydroxycineole was increased by 5.4-fold after optimizing codons for *E. coli* [130]. Modification of the *N*-terminal hydrophobic signal sequence is a common strategy for eukaryotic CYPs to decrease the formation of inclusion bodies [131]. This can be done by replacing the 15 *N*-terminal amino acids with the eight-residue hydrophilic "MALLLAVF" peptide from bovine in CYP71AV1 expressed by *E. coli*, leading to an 8-fold increase in the catalytic activity for dihydroartemisinic acid [132]. In addition, the "AKKTSSKGKL" peptide from rabbit, which was introduced to the *N*-terminus of AmI2′H from *Astragalus membranaceus* in *E. coli* [133], is an alternative choice. Most eukaryotic CYPs depend on inner membranes to achieve posttranslational modification, ER engineering expands the ER to provide more space for the correct folding of CYPs through the deletion or overexpression of regulatory genes. For example, the deletion of *PAF1*, which is responsible for encoding the phosphatidic acid phosphatase in *S. cerevisiae*, resulted in the obvious expansion of the ER and improved the expression of CYP716A12, CYP72A68, and CYP72A67. As a result, the titer of sapogenins *β*-amyrin, medicagenic acid and medicagenic-28-*O*-glucoside showed an 8-, 6-, and 16-fold increase, respectively [134]. Lastly, overexpression of *INO2* gene as a lipid-regulatory factor also led to the expansion of the ER and an 8-fold increase in the catalytic activity of CYP for protopanaxadiol [135].

Summary and outlook

The C–H and C=C oxygenation processes catalyzed by CYPs provide a convenient and efficient way to insert oxygen atoms into inert molecules. CYP-catalyzed C–H and C=C oxygenation reactions are widely applied in producing chemicals and pharmaceutical intermediates to activate cheap raw materials and insert O atoms in a single catalyst or multi-enzyme cascades. Using biotechnology methods, such as protein engineering, the catalytic efficiency of hydroxylation, epoxidation, and ketonization catalyzed by CYPs can be improved, and regioselectivity and enantioselectivity regulation are enhanced. To some extent, this provides more efficient catalysts and increases the synthetic applications of C–H and C=C oxygenation, especially for the synthesis of drug intermediates with lower cost and more straightforward process. In addition, with advancements in protein engineering technology, the new functions of CYPs have been further explored, such as the formation of C–C, C–N, C–B, and C–Si bonds via amination, alkylation, and carbine transfer [136,137]. Future efforts should focus on designing better CYPs from scratch for more challenging reactions via computer simulation. C–H and C=C oxygenation reactions, including hydroxylation, epoxidation, and ketonization, and various new functions catalyzed by CYPs will significantly contribute to agriculture, drug development, food and feed additives, and other fields.

CRediT authorship contribution statement

Yu Yan: Writing – original draft, Data curation. **Jing Wu:** Data curation. **Guipeng Hu:** Data curation. **Cong Gao:** Data curation. **Liang Guo:** Writing – review & editing. **Xiulai Chen:** Writing – review & editing. **Liming Liu:** Writing – review & editing. **Wei Song:** Writing – review & editing.

Declaration of competing interest

The authors declare no conflict of interest.

Acknowledgments

This work was financially supported by the National Key R&D Program of China (Grant No. 2021YFC2100100 and 2021YFC2102000); and the General Program of National Natural Science Foundation of China (Grant No. 22178146).

References

[1] Borgel J, Tanwar L, Berger F, Ritter T. Late-stage aromatic C-H oxygenation. J Am Chem Soc 2018;140:16026–31.
[2] Vijaykumar M, Punji B. Advances in transition-metal-catalyzed C-H bond oxygenation of amides. Synthesis-Stuttgart 2021;53:2935–46.
[3] Sang RC, Korkis SE, Su WQ, Ye F, Engl PS, Berger F, et al. Site-selective C-H oxygenation via aryl sulfonium salts. Angew Chem Int Ed 2019;58:16161–6.
[4] Bora P, Bora B, Bora U. Recent developments in synthesis of catechols by dakin oxidation. New J Chem 2021;45:17077–84.
[5] Farouk O, Ibrahim MA, El-Gohary NM. Synthesis, chemical reactivity and biological evaluation of the novel 2- (1-chloro-3-oxoprop-1-en-1-yl)amino -4-(4-methoxyphenyl)-6-*oxo*-1,6-dihydropyrimidine-5-carbonitrile. Synth Commun 2021;51:2991–3003.
[6] Shi C-Y, Li L, Kang W, Zheng Y-X, Ye L-W. Claisen rearrangement triggered by transition metal-catalyzed alkyne alkoxylation. Coord Chem Rev 2021;446:214131.
[7] Abdolalian P, Tizhoush SK, Farshadfar K, Ariafard A. The role of hypervalent iodine(iii) reagents in promoting alkoxylation of unactivated C(sp(3))-H bonds catalyzed by palladium(ii) complexes. Chem Sci 2021;12:7185–95.
[8] Vece V, Vuocolo G. Multicomponent synthesis of novel coelenterazine derivatives substituted at the C-3 position. Tetrahedron 2015;71:8781–5.
[9] Wang Y, Xie R, Huang L, Tian Y-N, Lv S, Kong X, et al. Divergent synthesis of unsymmetrical azobenzenes via Cu-catalyzed C-N coupling. Org Chem Front 2021;8:5962–7.
[10] Rao MLN, Ramakrishna BS. Rhodium-catalyzed directing-group-assisted aldehydic C-H arylations with aryl halides. Eur J Org Chem 2017;2017:5080–93.
[11] Grogan G. Hemoprotein catalyzed oxygenations: P450s, UPOs, and progress toward scalable reactions. J Am Chem Soc AU 2021;1:1312–29.
[12] Coleman T, Wong SH, Podgorski MN, Bruning JB, De Voss JJ, Bell SG. Cytochrome P450 CYP199A4 from *Rhodopseudomonas palustris* catalyzes heteroatom dealkylations, sulfoxidation, and amide and cyclic hemiacetal formation. ACS Catal 2018;8:5915–27.
[13] Wang X, Chen J, Ma N, Cong Z. Selective hydroxylation of alkanes catalyzed by cytochrome P450 enzymes. Hua Xue Xue Bao 2020;78:490–503.
[14] Chen J, Kong F, Ma N, Zhao P, Liu C, Wang X, et al. Peroxide-driven hydroxylation of small alkanes catalyzed by an artificial P450 BM3 peroxygenase system. ACS Catal 2019;9:7350–5.
[15] Zhang C, Liu PX, Huang LY, Wei SP, Wang L, Yang SY, et al. Engineering P450 peroxygenase to catalyze highly enantioselective epoxidation of *cis*-*β*-methylstyrenes. Chem Eur J 2016;22:10969–75.
[16] Arnold WR, Carnevale LN, Xie Z, Baylon JL, Tajkhorshid E, Hu H, et al. Anti-inflammatory dopamine- and serotonin-based endocannabinoid epoxides reciprocally regulate cannabinoid receptors and the TRPV1 channel. Nat Commun 2021;12:926.
[17] Hilberath T, Windeln LM, Decembrino D, Le-Huu P, Bilsing FL, Urlacher VB. Two-step screening for identification of drug-metabolizing bacterial cytochromes P450 with diversified selectivity. ChemCatChem 2020;12:1710–9.
[18] Semsary S, Crnovcic I, Driller R, Vater J, Loll B, Keller U. Ketonization of proline residues in the peptide chains of actinomycins by a 4-oxoproline synthase. ChemBioChem 2018;19:706–15.
[19] Jiang Y, Peng W, Li Z, You C, Zhao Y, Tang D, et al. Unexpected reactions of *α*,*β*-unsaturated fatty acids provide insight into the mechanisms of CYP152 peroxygenases. Angew Chem Int Ed 2021;60:24694–701.
[20] Buergler MB, Dennig A, Nidetzky B. Process intensification for cytochrome P450 BM3-catalyzed oxy-functionalization of dodecanoic acid. Biotechnol Bioeng 2020;117:2377–88.
[21] Wang Z, Shaik S, Wang B. Conformational motion of ferredoxin enables efficient electron transfer to heme in the full-length P450(TT). J Am Chem Soc 2021;143:1005–16.
[22] Kalita S, Shaik S, Kisan HK, Dubey KD. A paradigm shift in the catalytic cycle of P450: the preparatory choreography during O_2 binding and origins of the necessity for two protonation pathways. ACS Catal 2020;10:11481–92.
[23] Wang BJ, Li CS, Dubey KD, Shaik S. Quantum mechanical/molecular mechanical calculated reactivity networks reveal how cytochrome P450cam and its T252A mutant select their oxidation pathways. J Am Chem Soc 2015;137:7379–90.
[24] Wang J-b, Huang Q, Peng W, Wu P, Yu D, Chen B, et al. P450-BM3-catalyzed sulfoxidation versus hydroxylation: a common or two different catalytically active species? J Am Chem Soc 2020;142:2068–73.

[25] Cooper HLR, Groves JT. Molecular probes of the mechanism of cytochrome P450. oxygen traps a substrate radical intermediate. Arch Biochem Biophys 2011;507:111–8.
[26] Hammerer L, Winkler CK, Kroutil W. Regioselective biocatalytic hydroxylation of fatty acids by cytochrome P450s. Catal Lett 2018;148:787–812.
[27] Whitehouse CJC, Bell SG, Wong LL. P450 BM3 (CYP102A1): connecting the dots. Chem Soc Rev 2012;41:1218–60.
[28] Dietrich M, Do TA, Schmid RD, Pleiss J, Urlacher VB. Altering the regioselectivity of the subterminal fatty acid hydroxylase P450 BM3 towards gamma- and delta-positions. J Biotechnol 2009;139:115–7.
[29] Dubey KD, Wang BJ, Shaik S. Molecular dynamics and QM/MM calculations predict the substrate-induced gating of cytochrome P450 BM3 and the regio- and stereoselectivity of fatty acid hydroxylation. J Am Chem Soc 2016;138:837–45.
[30] Roberts AG, Katayama J, Kaspera R, Ledwitch KV, Trong IL, Stenkamp RE, et al. The role of cytochrome P450 BM3 phenylalanine-87 and threonine-268 in binding organic hydroperoxides. Biochim Biophys Acta Gen Subj 2016;1860:669–77.
[31] Malca SH, Scheps D, Kuehnel L, Venegas-Venegas E, Seifert A, Nestl BM, et al. Bacterial CYP153A monooxygenases for the synthesis of ω-hydroxylated fatty acids. Chem Commun 2012;48:5115–7.
[32] Notonier S, Gricman L, Pleiss J, Hauer B. Semirational protein engineering of CYP153A(M.aq.)-CPRBM3 for efficient terminal hydroxylation of short- to long-chain fatty acids. ChemBioChem 2016;17:1550–7.
[33] Li F, Ma L, Zhang X, Chen J, Qi F, Huang Y, et al. Structure-guided manipulation of the regioselectivity of the cyclosporine A hydroxylase CYP-sb21 from *Sebekia benihana*. Synth Syst Biotechnol 2020;5:236–43.
[34] Murataliev MB, Trinh LN, Moser LV, Bates RB, Feyereisen R, Walker FA. Chimeragenesis of the fatty acid binding site of cytochrome P450 BM3. replacement of residues 73-84 with the homologous residues from the insect cytochrome P450 CYP4C7. Biochemistry 2004;43:1771–80.
[35] Chen C-KJ, Shokhireva TK, Berry RE, Zhang H, Walker FA. The effect of mutation of F87 on the properties of CYP102A1-CYP4C7 chimeras: altered regiospecificity and substrate selectivity. J Biol Inorg Chem 2008;13:813–24.
[36] Chen C-KJ, Berry RE, Shokhireva TK, Murataliev MB, Zhang H, Walker FA. Scanning chimeragenesis: the approach used to change the substrate selectivity of fatty acid monooxygenase CYP102A1 to that of terpene ω-hydroxylase CYP4C7. J Biol Inorg Chem 2010;15:159–74.
[37] Cryle MJ, De Voss JJ. Facile determination of the absolute stereochemistry of hydroxy fatty acids by GC: application to the analysis of fatty acid oxidation by a P450 BM3 mutant. Tetrahedron: Asymmetry 2007;18:547–51.
[38] Scheps D, Malca SH, Richter SM, Marisch K, Nestl BM, Hauer B. Synthesis of ω-hydroxy dodecanoic acid based on an engineered CYP153A fusion construct. Microb Biotechnol 2013;6:694–707.
[39] Park H, Bak D, Jeon W, Jang M, Ahn J-O, Choi K-Y. Engineering of CYP153A33 with enhanced ratio of hydroxylation to overoxidation activity in whole-cell biotransformation of medium-chain 1-alkanols. Front Bioeng Biotechnol 2022;9:817455.
[40] Munday SD, Maddigan NK, Young RJ, Bell SG. Characterisation of two self-sufficient CYP102 family monooxygenases from *Ktedonobacter racemifer* DSM44963 which have new fatty acid alcohol product profiles. Biochim Biophys Acta Gen Subj 2016;1860:1149–62.
[41] Jang H-H, Shin S-M, Ma SH, Lee G-Y, Joung YH, Yun C-H. Role of Leu188 in the fatty acid hydroxylase activity of CYP102A1 from *Bacillus megaterium*. J Mol Catal B Enzym 2016;133:35–42.
[42] Baker GJ, Girvan HM, Matthews S, McLean KJ, Golovanova M, Waltham TN, et al. Expression, purification, and biochemical characterization of the flavocytochrome P450 CYP505A30 from *Myceliophthora thermophila*. ACS Omega 2017;2:4705–24.
[43] Cryle MJ, Espinoza RD, Smith SJ, Matovic NJ, De Voss JJ. Are branched chain fatty acids the natural substrates for P450 BM3? Chem Commun 2006;22:2353–5.
[44] Yasuda K, Sugimoto H, Hayashi K, Takita T, Yasukawa K, Ohta M, et al. Protein engineering of CYP105s for their industrial uses. Biochim Biophys Acta Proteins Proteom 2018;1866:23–31.
[45] McLean KJ, Hans M, Meijrink B, van Scheppingen WB, Vollebregt A, Tee KL, et al. Single-step fermentative production of the cholesterol-lowering drug pravastatin via reprogramming of penicillium chrysogenum. Proc Natl Acad Sci USA 2015;112:2847–52.
[46] Ke X, Sun J, Zheng Y. Construction and application of the high efficient electron transfer chain for cytochrome P450. Chem Life 2015;35:733–40.
[47] Saroay R, Roiban G-D, Alkhalaf LM, Challis GL. Expanding the substrate scope of nitrating cytochrome P450 TxtE by active site engineering of a reductase fusion. ChemBioChem 2021;22:2262–5.
[48] Wang X, Pereira JH, Tsutakawa S, Fang X, Adams PD, Mukhopadhyay A, et al. Efficient production of oxidized terpenoids via engineering fusion proteins of terpene synthase and cytochrome P450. Metab Eng 2021;64:41–51.
[49] Li SY, Podust LM, Sherman DH. Engineering and analysis of a self-sufficient biosynthetic cytochrome P450 PikC fused to the RhFRED reductase domain. J Am Chem Soc 2007;129:12940. -+.
[50] Negretti S, Narayan ARH, Chiou KC, Kells PM, Stachowski JL, Hansen DA, et al. Directing group-controlled regioselectivity in an enzymatic C-H bond oxygenation. J Am Chem Soc 2014;136:4901–4.
[51] Belsare KD, Ruff AJ, Martinez R, Shivange AV, Mundhada H, Holtmann D, et al. P-Link: a method for generating multicomponent cytochrome P450 fusions with variable linker length. Biotechniques 2014;57:13.
[52] Degregorio D, D'Avino S, Castrignano S, Di Nardo G, Sadeghi SJ, Catucci G, et al. Human cytochrome P450 3A4 as a biocatalyst: effects of the engineered linker in modulation of coupling efficiency in 3A4-BMR chimeras. Front Pharmacol 2017;8:121.
[53] Li SY, Du L, Bernhardt R. Redox partners: function modulators of bacterial P450 enzymes. Trends Microbiol 2020;28:445–54.
[54] Ciaramella A, Minerdi D, Gilardi G. Catalytically self-sufficient cytochromes P450 for green production of fine chemicals. Rendiconti Lincei Sci Fis Nat 2017;28:169–81.
[55] Wang YH, Lan DM, Durrani R, Hollmann F. Peroxygenases en route to becoming dream catalysts. what are the opportunities and challenges? Curr Opin Chem Biol 2017;37:1–9.
[56] Ramanan R, Dubey KD, Wang BJ, Mandal D, Shaik S. Emergence of function in P450-proteins: a combined quantum mechanical/molecular mechanical and molecular dynamics study of the reactive species in the H_2O_2-dependent cytochrome P450(SP alpha) and its regio- and enantioselective hydroxylation of fatty acids. J Am Chem Soc 2016;138:6786–97.
[57] Chen H, Moreau Y, Derat E, Shaik S. Quantum mechanical/molecular mechanical study of mechanisms of heme degradation by the enzyme heme oxygenase: the strategic function of the water cluster. J Am Chem Soc 2008;130:1953–65.
[58] Onoda H, Shoji O, Suzuki K, Sugimoto H, Shiro Y, Watanabe Y. α-Oxidative decarboxylation of fatty acids catalysed by cytochrome P450 peroxygenases yielding shorter-alkyl-chain fatty acids. Catal Sci Technol 2018;8:434–42.
[59] Matthews S, Tee KL, Rattray NJ, McLean KJ, Leys D, Parker DA, et al. Production of alkenes and novel secondary products by P450 OleT(JE) using novel H_2O_2-generating fusion protein systems. FEBS Lett 2017;591:737–50.
[60] Matthews S, Belcher JD, Tee KL, Girvan HM, McLean KJ, Rigby SEJ, et al. Catalytic determinants of alkene production by the cytochrome P450 peroxygenase OleT(JE). J Biol Chem 2017;292:5128–43.
[61] Fang B, Xu HF, Liu Y, Qi FX, Zhang W, Chen H, et al. Mutagenesis and redox partners analysis of the P450 fatty acid decarboxylase OleT(JE). Sci Rep 2017;7:44258.
[62] Du J, Liu L, Guo LZ, Yao XJ, Yang JM. Molecular basis of P450 OleT(JE): an investigation of substrate binding mechanism and major pathways. J Comput Aided Mol Des 2017;31:483–95.
[63] Wang JB, Lonsdale R, Reetz MT. Exploring substrate scope and stereoselectivity of P450 peroxygenase OleT(JE) in olefin-forming oxidative decarboxylation. Chem Commun 2016;52:8131–3.
[64] Belcher J, McLean KJ, Matthews S, Woodward LS, Fisher K, Rigby SEJ, et al. Structure and biochemical properties of the alkene producing cytochrome P450 OleTJE (CYP152L1) from the *Jeotgalicoccus* sp 8456 bacterium. J Biol Chem 2014;289:6535–50.
[65] Gartner A, Ruff AJ, Schwaneberg U. A 96-multiplex capillary electrophoresis screening platform for product based evolution of P450 BM3. Sci Rep 2019;9:15479.
[66] Iizaka Y, Arai R, Takahashi A, Ito M, Sakai M, Fukumoto A, et al. Engineering sequence and selectivity of late-stage C-H oxidation in the MycG iterative cytochrome P450. J Ind Microbiol Biotechnol 2022;49. kuab069.
[67] de Visser SP, Ogliaro F, Harris N, Shaik S. Multi-state epoxidation of ethene by cytochrome P450: a quantum chemical study. J Am Chem Soc 2001;123:3037–47.
[68] Guengerich FP. Cytochrome P450 oxidations in the generation of reactive electrophiles: epoxidation and related reactions. Arch Biochem Biophys 2003;409:59–71.
[69] Jin SX, Makris TM, Bryson TA, Sligar SG, Dawson JH. Epoxidation of olefins by hydroperoxo-ferric cytochrome P450. J Am Chem Soc 2003;125:3406–7.
[70] Sigmund M-C, Poelarends GJ. Current state and future perspectives of engineered and artificial peroxygenases for the oxyfunctionalization of organic molecules. Nat Catal 2020;3:690–702.
[71] Coleman T, Kirk AM, Chao RR, Podgorski MN, Harbort JS, Churchman LR, et al. Understanding the mechanistic requirements for efficient and stereoselective alkene epoxidation by a cytochrome P450 enzyme. ACS Catal 2021;11:1995–2010.
[72] Coleman T, Stok JE, Podgorski MN, Bruning JB, De Voss JJ, Bell SG. Structural insights into the role of the acid-alcohol pair of residues required for dioxygen activation in cytochrome P450 enzymes. J Biol Inorg Chem 2020;25:583–96.
[73] Liang JH, Wang HM, Bian XY, Zhang YM, Zhao GP, Ding XM. Heterologous redox partners supporting the efficient catalysis of epothilone B biosynthesis by EpoK in *Schlegelella brevitalea*. Microb Cell Fact 2020;19:180.
[74] Zhang W, Liu Y, Yan JY, Cao SN, Bai FL, Yang Y, et al. New reactions and products resulting from alternative interactions between the P450 enzyme and redox partners. J Am Chem Soc 2014;136:3640–6.
[75] Lucas D, Goulitquer S, Marienhagen J, Fer M, Dreano Y, Schwaneberg U, et al. Stereoselective epoxidation of the last double bond of polyunsaturated fatty acids by human cytochromes P450. J Lipid Res 2010;51:1125–33.
[76] Kubo T, Peters MW, Meinhold P, Arnold FH. Enantioselective epoxidation of terminal alkenes to (*R*)- and (*S*)-epoxides by engineered cytochromes P450 BM3. Chem Eur J 2006;12:1216–20.
[77] Yang Y, Cho I, Qi XT, Liu P, Arnold FH. An enzymatic platform for the asymmetric amination of primary, secondary and tertiary C(sp(3))-H bonds. Nat Chem 2019;11:987–93.
[78] Cho I, Prier CK, Jia ZJ, Zhang RK, Gorbe T, Arnold FH. Enantioselective aminohydroxylation of styrenyl olefins catalyzed by an engineered hemoprotein. Angew Chem Int Ed 2019;58:3138–42.
[79] Harada E, Murata J, Ono E, Toyonaga H, Shiraishi A, Hideshima K, et al. (+)-Sesamin-oxidising CYP92B14 shapes specialised lignan metabolism in sesame. Plant J 2020;104:1117–28.

[80] Deng Y, Weaver ML, Hoke KR, Pletneva EV. A heme propionate staples the structure of cytochrome c for methionine ligation to the heme iron. Inorg Chem 2019;58:14085–106.

[81] Hayashi T, Sato H, Matsuo T, Matsuda T, Hitomi Y, Hisaeda Y. Enhancement of enzymatic activity for myoglobins by modification of heme-propionate side chains. J Porphyr Phthalocyanines 2004;8:255–64.

[82] Geronimo I, Denning CA, Heidary DK, Glazer EC, Payne CM. Molecular determinants of substrate affinity and enzyme activity of a cytochrome P450 BM3 variant. Biophys J 2018;115:1251–63.

[83] Navapour L, Mogharrab N. In silico screening and analysis of nonsynonymous SNPs in human CYP1A2 to assess possible associations with pathogenicity and cancer susceptibility. Sci Rep 2021;11:4977.

[84] Grinkova YV, Denisov IG, McLean MA, Sligar SG. Oxidase uncoupling in heme monooxygenases: human cytochrome P450 CYP3A4 in nanodiscs. Biochem Biophys Res Commun 2013;430:1223–7.

[85] Zhao ZX, Lan DM, Tan XY, Hollmann F, Bornscheuer UT, Yang B, et al. How to break the janus effect of H_2O_2 in biocatalysis? understanding inactivation mechanisms to generate more robust enzymes. ACS Catal 2019;9:2916–21.

[86] Shoji O, Fujishiro T, Nishio K, Kano Y, Kimoto H, Chien SC, et al. A substrate-binding-state mimic of H_2O_2-dependent cytochrome P450 produced by one-point mutagenesis and peroxygenation of non-native substrates. Catal Sci Technol 2016;6:5806–11.

[87] Tripathi S, Li H, Poulos TL. Structural basis for effector control and redox partner recognition in cytochrome P450. Science 2013;340:1227–30.

[88] Batabyal D, Li H, Poulos TL. Synergistic effects of mutations in cytochrome P450cam designed to mimic CYP101D1. Biochemistry 2013;52:5396–402.

[89] Surawatanawong P, Tye JW, Hall MB. Density functional theory applied to a difference in pathways taken by the enzymes cytochrome P450 and superoxide reductase: spin states of ferric hydroperoxo intermediates and hydrogen bonds from water. Inorg Chem 2010;49:188–98.

[90] Sakalli T, Surmeli NB. Functional characterization of a novel CYP119 variant to explore its biocatalytic potential. Biotechnol Appl Biochem 2021. https://doi.org/10.1002/bab.2243.

[91] Ma NN, Chen ZF, Chen J, Chen JF, Wang C, Zhou HF, et al. Dual-functional small molecules for generating an efficient cytochrome P450 BM3 peroxygenase. Angew Chem Int Ed 2018;57:7628–33.

[92] Shoji O, Watanabe Y. Bringing out the potential of wild-type cytochrome P450s using decoy molecules: oxygenation of nonnative substrates by bacterial cytochrome P450s. Isr J Chem 2015;55:32–9.

[93] Shoji O, Watanabe Y. Monooxygenation of nonnative substrates catalyzed by bacterial cytochrome P450s facilitated by decoy molecules. Chem Lett 2017;46:278–88.

[94] Cane DE, Ikeda H. Exploration and mining of the bacterial terpenome. Acc Chem Res 2012;45:463–72.

[95] Crnovcic I, Ruckert C, Semsary S, Lang M, Kalinowski J, Keller U. Genetic interrelations in the actinomycin biosynthetic gene clusters of *Streptomyces antibioticus* IMRU 3720 and *Streptomyces chrysomallus* ATCC11523, producers of actinomycin X and actinomycin C. AABC 2017;10:29–46.

[96] Trefzer A, Jungmann V, Molnar I, Botejue A, Buckel D, Frey G, et al. Biocatalytic conversion of avermectin to 4"-oxo-avermectin: improvement of cytochrome P450 monooxygenase specificity by directed evolution. Appl Environ Microbiol 2007;73:4317–25.

[97] Wu K, Chen Y. Research progress on oxidoreductase mediated biocatalytic cascades. Chin J Synth Chem 2018;26:292–9.

[98] Mertens MAS, Thomas F, Noeth M, Moegling J, El-Awaad I, Sauer DF, et al. One-pot two-step chemoenzymatic cascade for the synthesis of a bis-benzofuran derivative. Eur J Org Chem 2019;2019:6341–6.

[99] Meng S, Guo J, Li Z, Nie K, Xu H, Tan T, et al. Enzymatic cascade biosynthesis reaction of musky macrolactones from fatty acids. Enzym Microb Technol 2019;131:109417.

[100] Loskot SA, Romney DK, Arnold FH, Stoltz BM. Enantioselective total synthesis of nigelladine a via late-stage C-H oxidation enabled by an engineered P450 enzyme. J Am Chem Soc 2017;139:10196–9.

[101] Chen J, Tang J, Xi Y, Dai Z, Bi C, Chen X, et al. Production of 14α-hydroxysteroids by a recombinant *Saccharomyces cerevisiae* biocatalyst expressing of a fungal steroid 14α-hydroxylation system. Appl Microbiol Biotechnol 2019;103:8363–74.

[102] Xiong X, Gou J, Liao Q, Li Y, Zhou Q, Bi G, et al. The Taxus genome provides insights into paclitaxel biosynthesis. Native Plants 2021;7:1026.

[103] Walls LE, Malci K, Nowrouzi B, Li RA, d'Espaux L, Wong J, et al. Optimizing the biosynthesis of oxygenated and acetylated Taxol precursors in *Saccharomyces cerevisiae* using advanced bioprocessing strategies. Biotechnol Bioeng 2021;118:279–93.

[104] Biggs BW, Rouck JE, Kambalyal A, Arnold W, Lim CG, De Mey M, et al. Orthogonal assays clarify the oxidative biochemistry of Taxol P450 CYP725A4. ACS Chem Biol 2016;11:1445–51.

[105] Sawayama AM, Chen MMY, Kulanthaivel P, Kuo M-S, Hemmerle H, Arnold FH. A panel of cytochrome P450 BM3 variants to produce drug metabolites and diversify lead compounds. Chem Eur J 2009;15:11723–9.

[106] Li A, Ilie A, Sun Z, Lonsdale R, Xu J-H, Reetz MT. Whole-cell-catalyzed multiple regio- and stereoselective functionalizations in cascade reactions enabled by directed evolution. Angew Chem Int Ed 2016;55:12026–9.

[107] Karande R, Salamanca D, Schmid A, Buehler K. Biocatalytic conversion of cycloalkanes to lactones using an in-vivo cascade in *Pseudomonas taiwanensis* VLB120. Biotechnol Bioeng 2018;115:312–20.

[108] Dennig A, Busto E, Kroutil W, Faber K. Biocatalytic one-pot synthesis of L-tyrosine derivatives from monosubstituted benzenes, pyruvate, and ammonia. ACS Catal 2015;5:7503–6.

[109] Ilie A, Lonsdale R, Agudo R, Reetz MT. A diastereoselective P450-catalyzed epoxidation reaction: anti versus syn reactivity. Tetrahedron Lett 2015;56:3435–7.

[110] Weaver-Guevara HM, Fitzgerald RW, Cote NA, Greenberg A. Cytochrome P450 can epoxidize an oxepin to a reactive 2,3-epoxyoxepin intermediate: potential insights into metabolic ring-opening of benzene. Molecules 2020;25:4542.

[111] Li A, Liu J, Pham SQ, Li Z. Engineered P450pyr monooxygenase for asymmetric epoxidation of alkenes with unique and high enantioselectivity. Chem Commun 2013;49:11572–4.

[112] Li A, Wu S, Adams JP, Snajdrova R, Li Z. Asymmetric epoxidation of alkenes and benzylic hydroxylation with P450tol monooxygenase from *Rhodococcus coprophilus* TC-2. Chem Commun 2014;50:8771–4.

[113] Yu D, Wang J-b, Reetz MT. Exploiting designed oxidase-peroxygenase mutual benefit system for asymmetric cascadereactions. J Am Chem Soc 2019;141:5655–8.

[114] Wu S, Liu J, Li Z. Organic synthesis via oxidative cascade biocatalysis. Synlett 2016;27:2644–58.

[115] Hu BD, Zhao XR, Wang ED, Zhou JW, Li JH, Chen J, et al. Efficient heterologous expression of cytochrome P450 enzymes in microorganisms for the biosynthesis of natural products. Crit Rev Biotechnol 2022. https://doi.org/10.1080/07388551.2022.2029344.

[116] Rosano GL, Morales ES, Ceccarelli EA. New tools for recombinant protein production in *Escherichia coli:* a 5-year update. Protein Sci 2019;28:1412–22.

[117] Milne N, Thomsen P, Knudsen NM, Rubaszka P, Kristensen M, Borodina I. Metabolic engineering of *Saccharomyces cerevisiae* for the de novo production of psilocybin and related tryptamine derivatives. Metab Eng 2020;60:25–36.

[118] Hausjell J, Schendl D, Weissensteiner J, Molitor C, Halbwirth H, Spadiut O. Recombinant production of a hard-to-express membrane-bound cytochrome P450 in different yeasts-comparison of physiology and productivity. Yeast 2020;37:217–26.

[119] Jin C-C, Zhang J-L, Song H, Cao Y-X. Boosting the biosynthesis of betulinic acid and related triterpenoids in *Yarrowia lipolytica* via multimodular metabolic engineering. Microb Cell Fact 2019;18:77.

[120] Zehentgruber D, Dragan C-A, Bureik M, Luetz S. Challenges of steroid biotransformation with human cytochrome P450 monooxygenase CYP21 using resting cells of recombinant *Schizosaccharomyces pombe*. J Biotechnol 2010;146:179–85.

[121] Theron CW, Labuschagne M, Albertyn J, Smit MS. Heterologous coexpression of the benzoate-*para*-hydroxylase CYP53B1 with different cytochrome P450 reductases in various yeasts. Microb Biotechnol 2019;12:1126–38.

[122] Wang CX, Su XY, Sun MC, Zhang MT, Wu JJ, Xing JM, et al. Efficient production of glycyrrhetinic acid in metabolically engineered *Saccharomyces cerevisiae* via an integrated strategy. Microb Cell Fact 2019;18:95.

[123] Chang T-s, Tsai Y-H. Inhibition of melanogenesis by yeast extracts from cultivations of recombinant *Pichia pastoris* catalyzing *ortho*-hydroxylation of flavonoids. Curr Pharmaceut Biotechnol 2015;16:1085–93.

[124] Zhao F, Bai P, Liu T, Li D, Zhang X, Lu W, et al. Optimization of a cytochrome P450 oxidation system for enhancing protopanaxadiol production in *Saccharomyces cerevisiae*. Biotechnol Bioeng 2016;113:1787–95.

[125] Miki Y, Asano Y. Biosynthetic pathway for the cyanide-free production of phenylacetonitrile in *Escherichia coli* by utilizing plant cytochrome P450 79A2 and bacterial aldoxime dehydratase. Appl Environ Microbiol 2014;80:6828–36.

[126] Yuan X, Rietzschel N, Kwon H, Walter Nuno AB, Hanna DA, Phillips JD, et al. Regulation of intracellular heme trafficking revealed by subcellular reporters. Proc Natl Acad Sci USA 2016;113:E5144–52.

[127] Park HA, Choi K-Y. α,Ω-Oxyfunctionalization of C12 alkanes via whole-cell biocatalysis of CYP153A from *Marinobacter aquaeolei* and a new CYP from *Nocardia farcinica* IFM10152. Biochem Eng J 2020;156:107524.

[128] Yadav R, Scott EE. Endogenous insertion of non-native metalloporphyrins into human membrane cytochrome P450 enzymes. J Biol Chem 2018;293:16623–34.

[129] Liu HM, Yuan M, Liu AM, Ren L, Zhu GP, Sun LN. A bifunctional enzyme belonging to cytochrome P450 family involved in the O-dealkylation and N-dealkoxymethylation toward chloroacetanilide herbicides in *Rhodococcus* sp. B2. Microb Cell Fact 2021;20:61.

[130] Wang X, Pereira JH, Tsutakawa S, Fang XY, Adams PD, Mukhopadhyay A, et al. Efficient production of oxidized terpenoids via engineering fusion proteins of terpene synthase and cytochrome P450. Metab Eng 2021;64:41–51.

[131] Pan Y, Abd-Rashid BA, Ismail Z, Ismail R, Mak JW, Ong CE. Heterologous expression of human cytochromes P450 2D6 and CYP3A4 in *Escherichia coli* and their functional characterization. Protein J 2011;30:581–91.

[132] Chen XX, Zhang CQ, Too HP. Multienzyme biosynthesis of dihydroartemisinic acid. Molecules 2017;22:1422.

[133] Chen J, Yuan H, Zhang L, Pan HY, Xu RY, Zhong Y, et al. Cloning, expression and purification of isoflavone-2'-hydroxylase from *Astragalus membranaceus* Bge. Var. mongolicus (Bge.) Hsiao. Protein Expr Purif 2015;107:83–9.

[134] Arendt P, Miettinen K, Pollier J, De Rycke R, Callewaert N, Goossens A. An endoplasmic reticulum-engineered yeast platform for overproduction of triterpenoids. Metab Eng 2017;40:165–75.

[135] Kim J-E, Jang I-S, Son S-H, Ko Y-J, Cho B-K, Kim SC, et al. Tailoring the *Saccharomyces cerevisiae* endoplasmic reticulum for functional assembly of terpene synthesis pathway. Metab Eng 2019;56:50–9.
[136] Liu Z, Arnold FH. New-to-nature chemistry from old protein machinery: carbene and nitrene transferases. Curr Opin Biotechnol 2021;69:43–51.
[137] Sarai NS, Levin BJ, Roberts JM, Katsoulis DE, Arnold FH. Biocatalytic transformations of silicon-the other group 14 element. ACS Cent Sci 2021;7:944–53.